Skewing For Both Cogging Torque Components In Permanent Magnet Machines

Devon R. McIntosh
Sonsight Inc.
17609 Clinton Dr., Accokeek, MD 20607
devonrocky@sonsightinc.com

Abstract: Cogging torque in permanent magnet motors and generators is characterized by a torque ripple that usually pulsates at a characteristically high angular frequency. Results of finite element (FE) analyses that show a previously unaddressed lower frequency cogging torque contribution that is superimposed on the higher frequency component was previously presented and analyzed. As cogging torque is minimized through successful application of optimization schemes, the relative proportion of the low-frequency component increases and becomes substantial. The current paper describes how a properly chosen skew angle can be used to decrease the amplitude of the high and/or low frequency cogging torque components. The approach is further demonstrated with the help of FE results from Comsol Multiphysics.

Keywords: coggging torque, permanent magnet motors, torque ripple, skewed rotor, skewed stator.

1. Introduction

Due largely to their high torque-to-current and torque-to-volume ratios, permanent magnet (PM) motors and generators are increasingly being used in a wide range of high performance applications such as industrial drives, robotics, computer peripherals, and automotive applications. However, most PM machines utilize a slotted iron structure with protruding teeth comprising the stator core that interacts with the PM poles on the rotor. This interaction generates a tendency for the rotor to align at preferential low energy detent positions relative to the stator slots. This is called cogging torque, and as the motor rotates, these torque fluctuations cause vibrations, noise and speed fluctuations. It can be a vital design consideration for machine startup and wherever accurate or constant speed motion control is required.

Cogging torque is proportional to the square of the magnetic field intensity, and is therefore increasingly problematic as PM's with higher residual magnetic fields are used. A number of techniques, supported by analytical and sometimes FE analysis and experimental results have been proposed and demonstrated for minimizing cogging torque [1] – [9]. These include optimizing the teeth width [1, 2, 3, 6], the pole width [2, 3, 4, 6, 7, 8], and the pole-to-teeth number ratio [2, 5, 6], and pairing teeth and poles of different widths [1, 2 and 4]. Also discussed are shaping the magnets [2, 7], notching the teeth [2, 4, 9], skewing the teeth or the poles [2, 4, 5, 7, 9], shifting the poles [4] and asymmetric motors [2]. Essentially all of these effects can be incorporated within a Fourier transformed air-gap field energy formulation described within several of the references and briefly reviewed below [1, 2, 3, 8].

A low frequency modulation of the cogging torque ripple, which can be significant, has been observed and analyzed [11]. The purpose of this paper is to numerically investigate the effect of skewing on the low frequency modulation as well as on both components. As such, the background on the cogging torque analysis is reviewed, then the effect of skewing on both cogging components is introduced, and then simple integrations of Comsol FE 2-D results are used to demonstrate the effects of utilizing different skew angles.

2. Cogging Without Skew

Cogging torque is generated by variations in the motor's magnetic field energy as the rotor turns. Since these energy variations are largely confined to the airgap and PM fields (i.e. the energy within the iron cores are typically considered negligible), the standard approach [1, 2, 3, 8, 11] is to examine the energy in these fields W_g due to the corresponding flux density distribution B_g, and as outlined in [1] and [2]:

$$W_g = \frac{1}{2\mu_0}\int B_g^2 dV \qquad (1)$$

More explicitly, for a radial flux machine with no skew, and therefore no variation in the axial (i.e. z)

direction (assuming PM permeability is the same as for air, and neglecting end effects):

$$W_g(\alpha) = \frac{L_A}{4\mu_0}(R_2^2 - R_1^2)\int_0^{2\pi} G^2(\theta) B_r^{'2}(\theta - \alpha) d\theta \qquad (2)$$

where:
α = rotational angle of the rotor,
θ = angular position around the machine
L_A = airgap length in axial direction,
For the external rotor machine, $R_2 = R_M$ and $R_1 = R_S$,
For the internal rotor machine, $R_2 = R_S$ and $R_1 = R_M$,
R_M = PM radius, and R_S = stator radius,
G(θ) = relative airgap permeance function (for instance, a simple functional form is to assume $G^2(\theta)$ is one constant value in the stator shoe areas and a smaller constant value in the stator slot areas, and both constant values are less than or equal to one [1, 2]),
$B_r^{'2}(\theta - \alpha)$ = modified PM remanence flux density (modified to include fringing field [3])

Cogging torque is given by :

$$T(\alpha) = -\frac{\partial W_g(\alpha)}{\partial \alpha} \qquad (3)$$

The standard form of $G^2(\theta)$ (i.e. the form the yields the high frequency component of cogging torque, which we shall here define as G_0^2) can be expanded using Fourier series [1,2, 8] as:

$$G_0^2(\theta) = \sum_{n=0}^{\infty} \left[G_{anNs} \cos nN_S\theta + G_{bnNs} \sin nN_S\theta \right] \qquad (4)$$

$B_r^{'2}(\theta - \alpha)$ can be likewise be expanded

$$B_r'^2(\theta - \alpha) = \sum_{n=0}^{\infty} \begin{bmatrix} B_{anNp} \cos nN_P(\theta - \alpha) \\ + B_{bnNp} \sin nN_P(\theta - \alpha) \end{bmatrix} \qquad (5)$$

N_S and N_P are the number of slots and the number of PM's respectively. For symmetric machines the sin terms in (4) and (5) are zero. Utilizing (4) within (2) yields $W_{g0}(\alpha)$:

$$W_{g0}(\alpha) = \frac{L_A}{4\mu_0}(R_2^2 - R_1^2)\int_0^{2\pi} G_0^2(\theta) B_r^{'2}(\theta - \alpha) d\theta \qquad (6)$$

Cogging torque can be determined by substituting the expansions (4) and (5) within (6), and then into (3) to obtain the cogging torque T_0 corresponding to the field energy $W_{g0.}$

$$W_{g0}(\alpha) = \frac{\pi L_A}{4\mu_0}(R_2^2 - R_1^2)\sum_{n=0}^{\infty} G_{anNL} B_{anNL} \cos nN_L\alpha \qquad (7)$$

$$T_0(\alpha) = \frac{\pi L_A}{4\mu_0}(R_2^2 - R_1^2)\sum_{n=0}^{\infty} nN_L G_{anNL} B_{anNL} \sin nN_L\alpha \qquad (8)$$

N_L is the least common multiple of N_S and N_P (i.e. LCM{N_S, N_P}).

As shown in [11], (7) and (8) describe only the high frequency cogging torque component. Incorporation of the low frequency component requires starting with a more general form for $G^2(\theta)$ obtained from a standard evaluation of the magnetic circuit along the flux path through the stator and rotor and across the airgap [10]. Such an expression for the gap flux B_g can be written as:

$$B_g = \frac{B_r}{1 + \frac{P_m}{P_g} + 4\frac{P_{ml}}{P_g}} \qquad (9)$$

where,
P_m = PM permeance
P_{ml} = magnet leakage permeance
P_g = airgap permeance

P_{ml} is associated with flux that leaks between adjacent magnets without going through the stator, and is modulated by the presence of the stator slots across the airgap. Only a fraction of the leakage flux ΔP_{ml} will vary with position relative to the slots, and together with a steady baseline value P_{ml0} comprise P_{ml} (i.e. $P_{ml}=P_{ml0}+ \Delta P_{ml}$). This is used within (9) to obtain:

$$\begin{aligned} B_g^2(\theta, \alpha) &= B_r^2(\theta - \alpha) G_0^2(\theta) - B_r^2(\theta - \alpha) G_1^2(\theta) \\ &= B_r^2(\theta - \alpha) G^2(\theta) \end{aligned} \qquad (10)$$

where,

$$G_1^2(\theta) = \frac{8\Delta P_{ml}(\theta)}{P_g} G_0^3(\theta) \qquad (11)$$

and,

$$G_0 = \left(1 + \frac{P_m + 4P_{ml0}}{P_g} \right)^{-1} \qquad (12)$$

As a specific example, consider the PM machine shown in Fig. 1 with $N_S = 7$ and $N_P = 9$. The magnet leakage flux varies over the nine magnets within the modeled quadrant. The quadrant constitutes the primary cell for this machine, so the leakage flux pattern must repeat within the next quadrant. Also, since it is the presence of the stator that generates the leakage flux variation, the leakage flux is a periodic function of θ with a fundamental period that is one quadrant long.

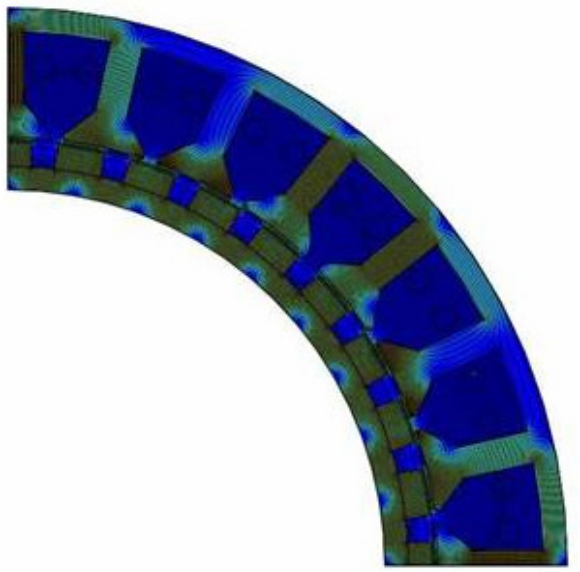

Fig 1. B-Field results from model of 7-Phase PM machine.

Since the period of ΔP_{ml} (which must be the same as that of the leakage flux) must be an integral multiple of the period of G_0^3, the periodicity of G_1^2 is determined by that of ΔP_{ml} (i.e. the longest period). Substituting (10) into (1) yields:

$$W_g(\alpha) = W_{g0}(\alpha) - \left[\frac{1}{4\mu_0} L_A (R_2^2 - R_1^2) \cdot \int_0^{2\pi} G_1^2(\theta) B_r^{'2}(\theta - \alpha) d\theta \right] \quad (13)$$

or,

$$W_g(\alpha) = W_{g0}(\alpha) - W_{g1}(\alpha)$$

Similar to (4), we expand G_1^2:

$$G_1^2(\theta) = \sum_{n=0}^{\infty} \left[G'_{anNc} \cos nN_c\theta + G'_{bnNc} \sin nN_c\theta \right] \quad (14)$$

where,

$N_C = GCF\{N_P, N_S\}$ = number of primary cells (in this case 4)

GCF = Greatest Common Factor

Similar to (7), substitution into (13) yields:

$$W_{g1}(\alpha) = \frac{\pi L_A}{4\mu_0} (R_2^2 - R_1^2) \sum_{n=0}^{\infty} G'_{anNP} B_{anNP} \cos nN_P\alpha \quad (15)$$

By definition, $N_P = LCM\{N_C, N_P\}$.

Substitution of (13) with (15) into (3) gives the total torque:

$$T(\alpha) = T_0(\alpha) + T_1(\alpha)$$

where,

$$T_1(\alpha) = -\frac{\pi L_A}{4\mu_0} (R_2^2 - R_1^2) \sum_{n=0}^{\infty} nN_P G'_{anNP} B_{anNP} \sin nN_P\alpha \quad (16)$$

2. Cogging With Skew

For skewing of the stator teeth and slots, G_0^2 in (4) (as described in [2]) and G_1^2 in (14) for symmetric machines, become respectively:

$$G_0^2(\theta, z) = \sum_{n=0}^{\infty} G_{anNs} \cos nN_s \left(\theta - \frac{\alpha_s}{L_A} z \right) \quad (17)$$

and

$$G_1^2(\theta, z) = \sum_{n=0}^{\infty} G'_{anNc} \cos nN_c \left(\theta - \frac{\alpha_s}{L_A} z \right) \quad (18)$$

α_s is the skew angle.

For skewing of the PM's, $B_r^{'2}(\theta - \alpha)$ in (5) for symmetric machines, becomes:

$$B_r'^2(\theta - \alpha, z) = \sum_{n=0}^{\infty} B_{anNp} \cos nN_P(\theta + \frac{\alpha_s}{L_A} z - \alpha) \quad (19)$$

Similar cogging torques are obtained with either a skewed stator (i.e. (17) and (18)) or a skewed rotor (19). Inserting (19) into (10), and (10) into (1) gives,

$$W_g(\alpha) = \frac{\pi}{4\mu_0}(R_2^2 - R_1^2) \bullet \int_{-\frac{L_A}{2}}^{\frac{L_A}{2}} dz \sum_{n=0}^{\infty} \left[\begin{array}{l} G_{anNL} B_{anNL} \cos nN_L \left(\frac{\alpha_s z}{L_A} - \alpha \right) \\ -G'_{anNP} B_{anNP} \cos nN_P \left(\frac{\alpha_s z}{L_A} - \alpha \right) \end{array} \right] \quad (20)$$

The dz integral gives:

$$W_g(\alpha) = \frac{\pi L_A}{2\mu_0 \alpha_s}(R_2^2 - R_1^2) \bullet \sum_{n=0}^{\infty} \left[\begin{array}{l} \frac{1}{nN_L} G_{anNL} B_{anNL} \sin(nN_L \frac{\alpha_s}{2}) \cos nN_L \alpha \\ -\frac{1}{nN_P} G'_{anNP} B_{anNP} \sin(nN_P \frac{\alpha_s}{2}) \cos nN_P \alpha \end{array} \right] \quad (21)$$

The first and second terms in the summation are the high and low frequency contributions respectively. Using (3), the torque is:

$$T(\alpha) = \frac{\pi L_A}{2\mu_0 \alpha_s}(R_2^2 - R_1^2) \bullet \sum_{n=0}^{\infty} \left[\begin{array}{l} G_{anNL} B_{anNL} \sin(nN_L \frac{\alpha_s}{2}) \sin nN_L \alpha \\ -G'_{anNP} B_{anNP} \sin(nN_P \frac{\alpha_s}{2}) \sin nN_P \alpha \end{array} \right] \quad (22)$$

Equation (22) shows that for either the high or the low frequency components, there is no cogging torque of that component when the skew angle is an integer multiple of the corresponding fundamental cogging torque period (i.e. for n = 1). Moreover, both high and low frequency components will disappear if α_s is an integer multiple of the fundamental low frequency period since by definition, N_P is an integer multiple of N_L. i.e.:

$T(\alpha) = 0$ for $\alpha_s = 2m\pi/N_P$

It may be easier to manufacture the rotor with skew arranged in discrete steps as shown in Fig. 2, which show the stepped PM's. To illustrate the differences between this and a continuous skew, the cogging torque of a FE model similar to that shown in Fig. 1 was calculated with Comsol Multiphysics AC/DC Module, and the effect of skew approximated by utilizing (20) within (3), and replacing the dz integral in (20) with k discrete sums, where k represents the number of discrete levels in a stack of PM's, where each level is shifted relative to the next. For instance, in Fig. 2, k = 2, and the step angle is half the skew angle (as dictated by the summation in (20)). The results are shown in Fig.'s 3 and 4. Fig. 3 shows the result of skew for k = 12, which is essentially a continuous skew. HFSkewC has $\alpha_s = 2\pi/N_L$, which as expected almost eliminates the high frequency cogging component, but not the low frequency component. LFSkewC has $\alpha_s = 2\pi/N_P$, which essentially eliminates both cogging components.

Fig. 4 shows the result of skew for k = 2, which is the case shown in Fig. 2. HFSkewD has a step angle of $m\pi/N_L$, which greatly reduces the high frequency cogging component, but not the low frequency component, and LFSkewD has a step angle of $m\pi/N_P$, which does reduce both components. The stepped k=2 high frequency skew (i.e. HFSkewD) is almost as effective as the corresponding continuous skew.

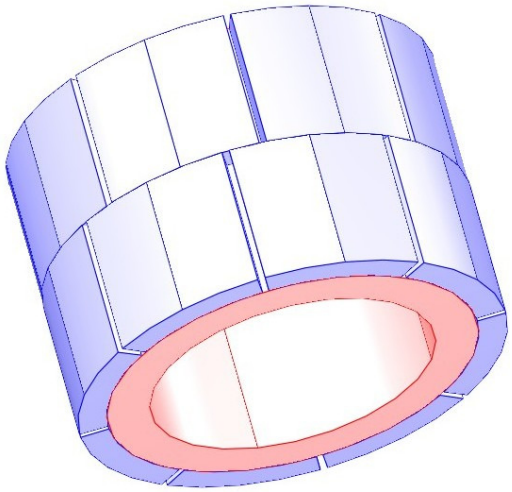

Fig. 2. Rotor showing a two level stack of PM's (i.e. k=2) with the levels offset by a step angle of half of what the skew angle would be.

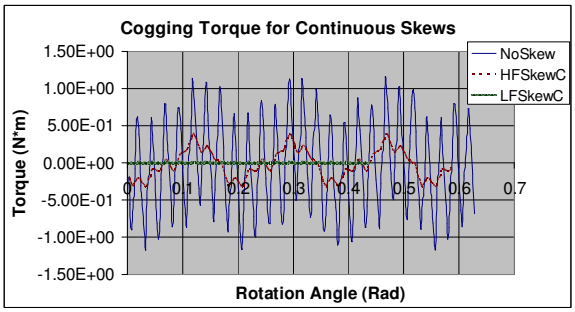

Fig. 3. LFSkewC has $\alpha_s = 2\pi/N_P$, and HFSkewC has $\alpha_s = 2\pi/N_L$

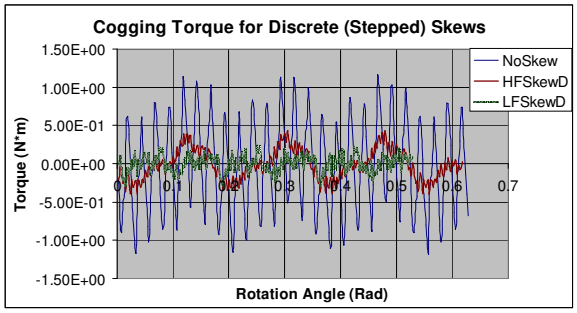

Fig. 4. Both skews are stepped with k = 2 as shown in Fig. 2. The step angle for LFSkewD is π/N_P, and that for HFSkewD is π/N_L.

3. Use of COMSOL Multiphysics

The problem modeled in COMSOL is similar to a combination of two examples from the AC/DC Model Library: the *Generator in 2D*, and the *Generator with Mechanical Dynamics and Symmetry*; therefore, the governing E-M equation is the same quasi-static approximation used in those models. Only 1/4th of the generator is modeled; the boundary conditions are the same as that of the latter model. However, a prescribed rotation exactly as described in the former model was used.

4. Conclusion

Skew was incorporated within a formulation used to describe both the high and the low frequency components of cogging torque in PM machines, and showed that for either the high or the low frequency components, there is no cogging torque of that component when the skew angle is an integer multiple of the corresponding fundamental cogging torque period (i.e. for n = 1). Moreover, both high and low frequency components will disappear if the skew angle is an integer multiple of the fundamental low frequency period.

The effect of various types of skew on both high and low frequency cogging torque components was numerically characterized, and the ability to simultaneously eliminate both high and low frequency cogging torque components demonstrated.

Acknowledgement

This project was supported by the Small Business Innovation Research program of the USDA National Institute of Food and Agriculture (NIFA), Grant Number 2009-33610-19884.

References

1. S.M. Hwang, J.B. Eom, G.B.Hwang, W.B. Jeong, and Y.H. Jung, "Cogging Torque and Acoustic Noise Reduction in Permanent Magnet Motors by Teeth Pairing", *IEEE Trans. Mag*., **vol. 36**, No. 5, pp. 3144-3146, (2000).
2. S.M. Hwang, J.B. Eom, D.W. Lee, and B.S. Kang, "Various Design Techniques to Reduce Cogging Torque by Controlling Energy Variation in Permanent Magnet Motors", *IEEE Trans. Mag*., **vol. 37**, No. 4, pp. 2806-2809, (2001).
3. B. Ackerman, J.H.H. Janssen, R. Sottek, R.I. van Steen, "New technique for reducing cogging torque in a class of brushless DC motors", *IEEE Proc.*-B, **vol. 139**, No. 4, pp. 315-320, (1992).
4. N. Bianchi and S. Bolognani, "Design technique for reducing the cogging torque in sorface-mounted PM Motors", *IEEE Trans. Ind. Appl.,* **vol. 38**, No. 5, pp. 1259-1265, (2002).
5. D.C. Hanselman, "Effect of skew, pole count and slot count on brushless motor radial force, cogging torque and back EMF", *IEEE Proc.-Electr. Power Appl.*, **vol. 144**, No. 5, pp. 325-330, (1997).
6. C.C. Hwang, S.B. John, and S.S. Wu "Reduction of cogging torque in spindle motors for CD-ROM drive", *IEEE Trans. Mag*., **vol. 34**, No. 2, pp. 468-470, (1998).
7. A. Kumar, S. Marwaha, A. Marwaha, "Comparison of methods of minimization of cogging torque in wind generators using FE analysis", *J. Indian Inst. Sci.*, **vol. 86**, pp. 355-362, (2001).
8. Y. Yang, X. Wang, R. Zhang, T. Ding, R. Tang, "The optimization of pole arc coefficient to reduce coging torque in surface-mounted permanent magnet motors", *IEEE Trans. Mag*., **vol. 42**, No. 4, pp. 1135-1138, (2006).
2. S. Hwang, and D.K. Lieu, "Design techniques for reduction of reluctance torque in brushless in permanent magnet motors", *IEEE Trans. Mag*., **vol. 30**, No. 6, pp. 4287-4289, (1994).
10. D.C. Hanselman, *Brushless Permanent-Magnet Motor Design*, pp. 64-67. McGraw-Hill, New York (1994).
11. D.R. McIntosh, "Identification and Analysis of Low-Frequency Cogging Torque Component in Permanent Magnet Machines", *Comsol Multiphysics Conference Proceedings*, Boston (2008).